Surface Characteristics Improvement of AZ31B Magnesium by Surface Compositing with Carbon Nano-tubes through Friction Stir Processing

M. Soltani
Department of Materials Engineering,
Isfahan University of Technology, Iran,
E-mail: maad.soltani@ma.iut.ac.ir
*Corresponding author

M. Shamanian, B. Niroumand
Department of Materials Engineering,
Isfahan University of Technology, Iran, E-mail: shamanian@cc.iut.ac.ir, behzn@cc.iut.ac.ir

Received: 29 October 2014, Revised: 15 December 2014, Accepted: 20 December 2014

Abstract: In this research, compositing the surface of AZ31B magnesium alloy with CNT was studied by FSP. The investigated parameters were rotational speed (500-1500 rpm), transverse speed (12-44 mm/min), number of passes (1-4), and CNT weight fraction (0-2%). Microhardness testing, optical metallography, FESEM, and EDS analysis were used for the characterization of the samples. The suitable limits for the transverse speed and rotational speed were 12-24 mm/min and 870-1140 rpm, respectively. The highest hardness in the FSP without compositing was observed at the transverse speed of 24 mm/min, rotational speed of 870 rpm with a hardness of about 60 Vickers, and the stir region grain size of less than 5 μm. The Zener-Holman parameter was calculated and the least value was related to the conditions of the transverse speed of 12-24 mm/min and rotational speed of 870 rpm; as a result, the samples with the finest grain size were theoretically and experimentally marked. The most homogenous structure with the highest hardness was related to the three-pass processed sample with a hardness of 69 Vickers. The best rate of CNT weight was 2%, enjoying the highest hardness. The FESEM images confirmed the suitable distribution of CNTs in matrix after the performance of the three-pass processing.

Keywords: Carbon Nano Tube (CNT), Friction Stir Processing (FSP), Surface Composite, Zener-Holloman Parameter

Reference: Soltani, M., Shamanian, M., and Niroumand, B., "Improvement of the Surface Characteristics of AZ31B Magnesium by Surface Compositing with Carbon Nano-Tubes through Friction Stir Processing", Int J of Advanced Design and Manufacturing Technology, Vol. 8/No. 1, 2015, pp. 85-95.

Biographical notes: M. Soltani is MSc student, studying Materials Engineering at the Department of Materials Engineering, Isfahan university of Technology, Isfahan, Iran. His current research interest includes Friction Stir Processing. **M. shamanian and B. Niroumand** are faculty members of Materials Engineering Department at Isfahan University of Technology, Iran. Their current research interests focus on Friction Stir processing and welding, Casting.

1 INTRODUCTION

Due to low density and high specific strength, magnesium alloys enjoy high potentiality for being used in aviation and car industries [1]. Unfortunately, magnesium also exhibits some unfavourable properties including weak resistance to corrosion and wear, low resistance to creep, high chemical activity, low hardness and tensile strength, and low flexibility [2]. These factors prevent the increasing application of this metal. Hardness and wear resistance of these alloys are very low compared to other metals. Researches have shown that by shape modification and grain size reduction, the mechanical properties of these metals and their alloys may be improved [1].

One of the economical approaches to the optimal use of materials is using substrates of low mechanical properties and surfaces of higher ones. Surface compositing is one of methods of improving surface properties in which a material with normal mechanical properties is composited through different methods like FSP with reinforcing by materials such as oxide, carbide, and nitride particles as well as carbon nanotube, etc. [3]. Therefore, a hard surface with higher mechanical properties and wear resistance is obtained. Some research activities have been performed on the FSP of magnesium alloys for different purposes.

Most of these researches have been carried out on the most well-known group of magnesium alloys, i.e. the wrought alloys of AZxx (magnesium, aluminium, and zinc [4]. Woo et al., [4] embarked on the study of the differences in textures and the effect of these textures on the tensile behaviour of FSP AZ31 of magnesium alloy. They found out that FSP had a significant effect on texture in magnesium alloys and texture difference in the FSP and the transitional regions had a great effect on mechanical properties. The correlation between texture and tensile test results proposed that the severe texture dissimilarity during FSP considerably affects tensile behaviour of the FSP magnesium alloy.

Darras presented a model for the prediction of gain size in FAC AZ31 magnesium alloy which was capable of predicting the average grain size of a FS-processed material among process parameters [5]. The suggested model was used for both dynamic recrystallization and grain growth. In his view, one of the most important reasons preventing the extensive use of ESP and effective modification of the microstructure is the lack of tools for prediction and correct selection of the parameters to attain the desirable grain size. Du et al., embarked on the production of nanostructure FSP AZ61 alloy by a two-pass method [6]. They were able to reach a 100-nonometer gain size on the surface with a final hardness of about 3 times more than that of the base metal. Their proposed mechanism for the production of nanostructures was recrystallization at two FSP stages. In another research, Woo et al., studied the nanostructure, texture, and the residual stress in FSP AZ31 alloy [7]. They found out that although FSP did not cause significant changes in hardness and chemical composition of FSP region and region affected by heat, however it left significant effects on the tensile strength, texture, and the residual stresses. They studied the relation between texture changes and reduction in tensile strength as well as its effect on the reduction of the residual stress in the stir region.

Some researchers have also been conducted on some alloys of AZxx family including AZ91 and AZ61 in the area of compositing. Faraji et al., examined the effect of the process parameters on the microstructure and hardness of AZ91/Al_2O_3 composite layer produced by FSP method [8]. Researches on hardness have shown that the combination of nano and micro size Al_2O_3 particulates in magnesium matrix resulted in a coincident increase in hardness. In another research work, Asadi et al., embarked on the production of AZ91/SiC composite layer by FSP method [9]. Results revealed that FSP is an effective process to produce SiC/AZ91 composite layer with even spreading of SiC particles, good interfacial integrity and substantial grain refinement. Also, in another research performed by Asadi et al., the effect of the type of nanoparticles and the number of process passes on the nano-composites produced by FSP method was investigated [10]. Lee et al., produced a nano-composite by the FSP method using SiO2 nanoparticles (by %5-%10 volume) in a substrate of AZ61 alloy [11]. Regarding the base metal, the hardness of the composites approximately doubled and exhibited high strain rate superplasticity.

The phenomenon of surface compositing for the improvement of the mechanical properties of metallic sheets is advancing forward and as it was mentioned above, the use of nanometre reinforcing materials for this purpose has already started in recent years. Due to the properties such as very high ratio of surface to volume, superconductivity, pinning of the grain boundaries, hardness improvement, and mechanical properties, carbon nanotubes (CNTs) enjoy high potentiality for being used in surface compositing. Although no article has yet been published concerning surface compositing of magnesium alloys by CNT, while dealt with in the current investigation, some articles have been published regarding surface compositing of aluminum alloys by CNT through FSP method [3], [12-14].

With regard to what was mentioned above, a detailed and serious study of surface compositing of AZ31B alloy by CNT has not yet been conducted precisely. The present study, therefore, tackles examining of surface compositing of AZ31B magnesium alloy by CNT and investigating the effect of the four parameters

of advancing speed of tools, rotational speed of tools, CNT weight percentage, the number of passes on grain grading, and mechanical properties of composite as well.

2 EXPERIMENTAL PROCEDURE

The initial material used in this research was the extruded alloy of AZ31B magnesium with a width and thickness of 80 mm by 20 mm, respectively, from which samples with a dimension of 100 mm × 40 mm × 8 mm were prepared. The extruded alloy of AZ31B magnesium is from the group of solid solution and hardening precipitation alloys [11]. The approximate chemical composition of the sheet was identified by EDS analysis and its average value is presented in Table 1 [15].

Table 1 Chemical composition of AZ31B magnesium by EDS method

El	Mg	Al	Zn	Si	Ca	Fe	Ni	Cu	Mn
Wt %	94.33	3.61	1.03	0.57	0.13	0.16	0.07	0.09	0.02

The purchased reinforcer employed in this research was a multi-wall carbon nanotube (MWCNT) with a purity of %95, an external diameter of 20-30 nm, an internal diameter of 5-10 nm, a length of 10-30 μm, and a specific area of 110 m^2/g, with a CVD synthesis method manufactured by Neutrino Company. The SEM image of these nanotubes is presented in Fig. 1 (a). The employed pin was of AISI H13 steel (DIN 1.2344). The pin went under standard hardening heat treatment after preparation and milling [16], and its hardness reached about 45 HRC. The final shape of the pin is depicted in Fig. 1 (b).

The end diameter, shoulder diameter, the height, and diameter of the tool were 15 mm, 18 mm, 5 mm, and 6 mm, respectively and the pitch of the pin was 1 mm with its turn to the right. Based on the previous studies, the reason for the use of pitched pin is producing distortion and more fluidity of the matter during the process [3], [17], and [18]. A milling machine was employed for this purpose and the sample was firmly kept by a fixture.

Before the start of each test, the surface of the sample was properly cleaned and decreased by alcohol and Aston. The nanotubes were then placed inside grooves with a width and depth of 1 mm and 4 mm, respectively over the surface of the sample. To close the grooves and prevent the exit of CNTs at FSP stage, pin-free (shoulder) devices were used and moved over the sample once (at transverse speed of 24 mm/min and rotational speed of 870 rpm). At the next stage, the same work was performed by the use of the original pin under specific conditions, while compressed air was blown under the piece for cooling.

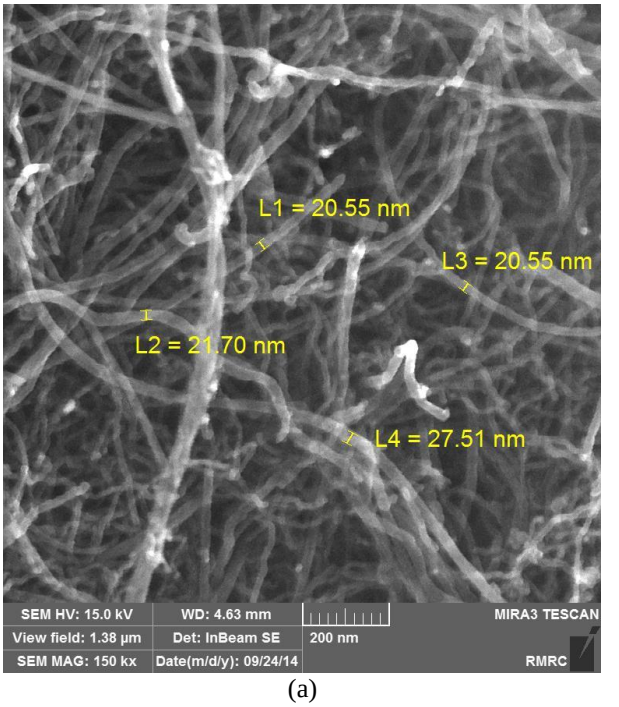

(a)

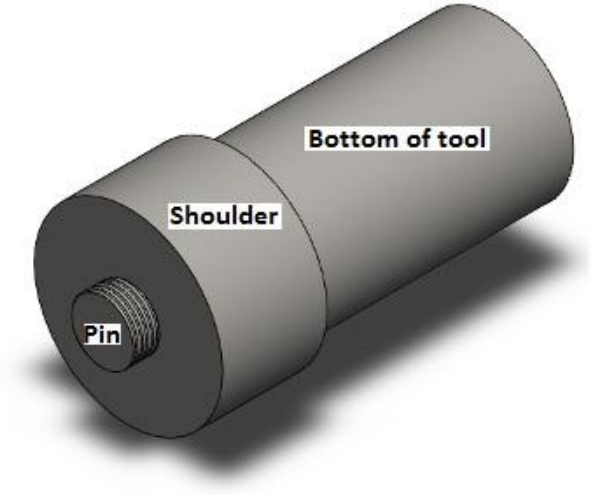

(b)

Fig. 1 Image (a) shows a SEM image of the carbon nanotubes, and image (b) is the schematic image of the pitched pin used in this research

In some references, the presence of the cooling source has resulted in improving of mechanical properties [19]-[21]. The penetration depth of the tool shoulder was selected to be 0.1 mm with the tool deviation angle of 2 degrees. The pin rotational direction was selected to be right-turning, since the left-turning direction

would cause the surface of the piece develop tunnel defect.

The parameters under study were rotational speed (879-140 rpm), transverse speed (12-24 mm/min), CNT weight fraction (up to 2% by weight), and the number of passes (1-3 passes) extracted from different sources. The volume and weight of the composite region was first specified for determining the employed CNT weight (shown in Fig. 2 (a)). By performing the computations related to volume and having the density of the material (1.77 gr/cm^3 for AZ31B alloy), the suitable CNT weight can be calculated. As it is observed in Fig. 2, the *S* region is the compositing region composed of two rectangular cubes. It should be noted that after the FSP operations, the extent of the FSP region might get a bit larger due to local melting, bringing about a minor error in the percentage of the reinforcing material. The schematic image of the sample before and after FSP is depicted in Fig. 2 (b).

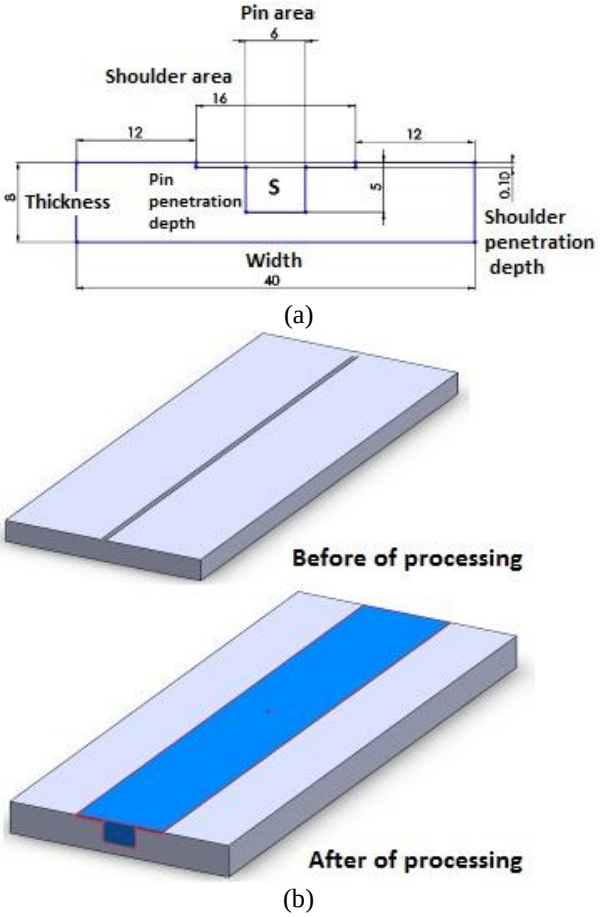

Fig. 2 Image (a) shows the schematic image of the region under FSP, and image (b) is the sample before and after FSP with nanotubes

After carrying out the tests, the cross-section of some samples were prepared and micro-hardness test and metallography test were performed. Seven hardness tests were taken on each sample in the nugget region and average value was registered. To study their microstructures, samples were polished by a 4000-mesh emery and polished with alumina powder. The etch solution contained 4.2 grams of picric acid, 10 millilitres of acetic acid, 70 millilitres of ethanol, and 10 millilitres of distilled water [19]. The sample was immersed in the etch solution for 30 to 60 seconds. Imaging was done by optical microscope (Nikon Epiphot 300) and micro-hardness testing was performed by Vickers method with a 50-gram load from a distance of 1 millimetre from the surface by application of a 20-second of load (Buehler Micromet 5101). The surfaces of the selected samples were analyzed by FESEM, where some regions were analyzed by EDS to determine the chemical analysis.

3 RESULTS AND DISCUSSIONS

Study of raw sample

The hardness of raw sample was 55.3 HV after hardness testing. The optical metallography images of the raw sample are presented in Fig. 3(a) and (b). A significant point in images (a) and (b) is the presence of a series of paths with different colour contrasts. These paths were not present in the sample before metallography and were not removed by the repetition of polishing and etching operations. These paths were probably created due to etching process as a result of different residual stresses of the previous forming process. This process could be rolling or extrusion which leads to directionality of the structure. It seems that this structural directionality has led to gradual corrosion during etching process and easier corrosion of bold-colored paths with little corrosion of the pale-colored paths. FESEM imaging and EDS analysis were performed to ensure the validity of this hypothesis (Fig. 3(c) to (e)).

First stage tests (FSP without compositing)

The first stage tests were performed to specify the precise limit of initial parameters (within the range of transverse speed of 12-44 mm/min and rotational speed of 550-1500 rpm) so as to ensure the lack of defects such as tunnelling, melting, decline of properties, etc. These tests were performed in one pass. It was specified at this stage that in case of left-turning pin, an open-end tunnel defect is created. If the pin turns right, the fluidity of the material gets upward and neutralized by tool shoulder.

It was also specified at this stage that the rotational speeds of 500 and 660 rpm as well as the transverse speeds of 32-44 mm/min do not create the semi-solid state; the modification of grain does not take place properly, and the alloy severely sticks to the pin body

due to the insufficient heat created. At the transverse speeds of less than 12 mm/min and rotational speeds of above 1140 rpm, a state of melting is generated in the piece while the inlet heat is very high.

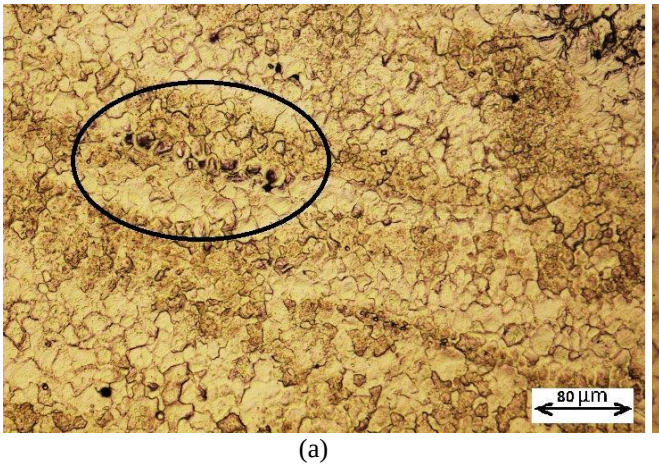

(a)

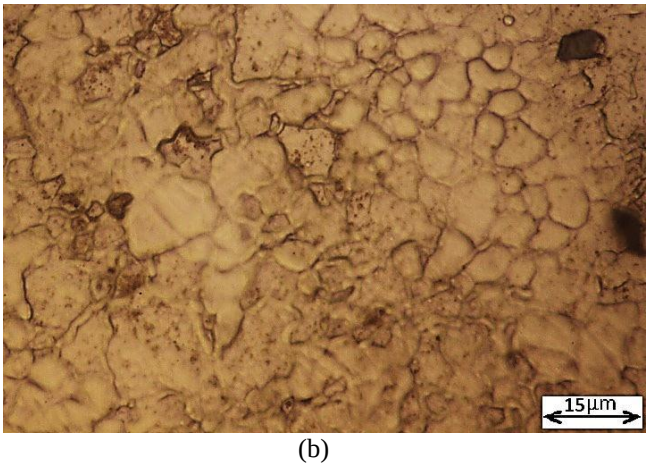

(b)

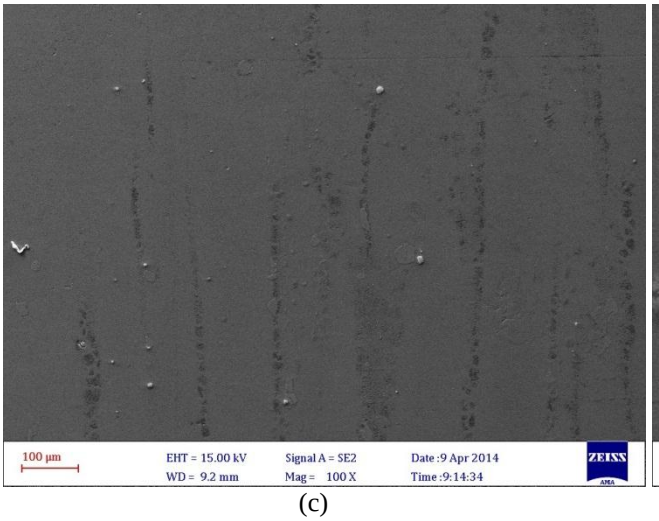

(c)

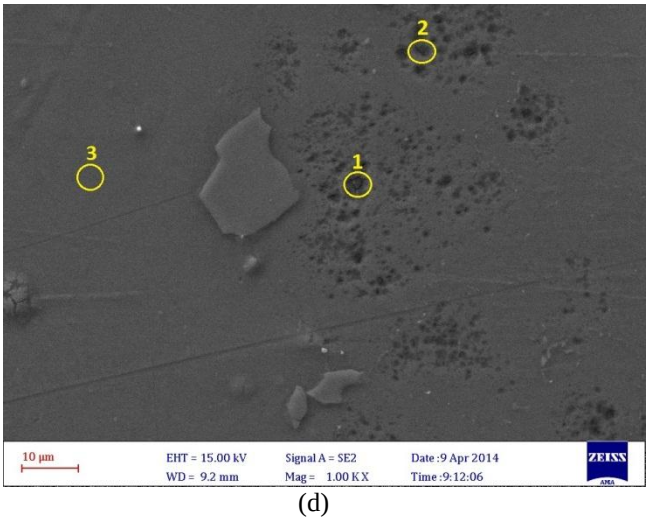

(d)

EDS 3

Element	Wt%	Error%
Mg	68.0	0.5
O	16.5	0.3
C	6.2	0.5
Al	5.7	0.2
Zn	3.7	0.3

(e)

EDS 2

Element	Wt%	Error%
Mg	75.2	0.5
O	11.7	0.3
C	5.7	0.4
Al	4.6	0.2
Zn	2.7	0.3

(f)

EDS 3

Element	Wt%	Error%
Mg	97.7	0.4
O	0.5	0.1
C	2.4	0.3
Al	2.4	0.2

(g)

Fig. 3 (a) and (b) are optical metallography images of the raw sample with different magnifications; (c) and (d) are FESEM images of the raw sample surface; and (e) and (f) are EDS elemental analyses of the raw sample surface (the numbers specified in image (d)).

At the end of this stage it was specified that the acceptable results were monitored at conditions of 870 rpm and 24 mm/min. The relevant results of the hardness tests are presented in Table 2 and metallographic images are shown in Fig. 4. As it is observed in Table 2, the best results are obtained within the range of the transverse speeds of 12-24 mm/min and rotational speeds of 870-1140 rpm. Therefore, this range was selected for the continuation of the study. The stir region is properly grain refined in samples A-1 and A-2 and it could be said that the average size of grains is less than 5 µm. On the other hand, the grain growth is seen in HAZ where, probably a recrystallization has also taken place. The size of the

grains in the stir region of sample A-6 is about 10 μm which is larger than those in samples A-1 and A-2. It may be concluded that the grain growth has also taken place after the recrystallization in the stir region, and due to the inlet heat, the grains in HAZ have grown.

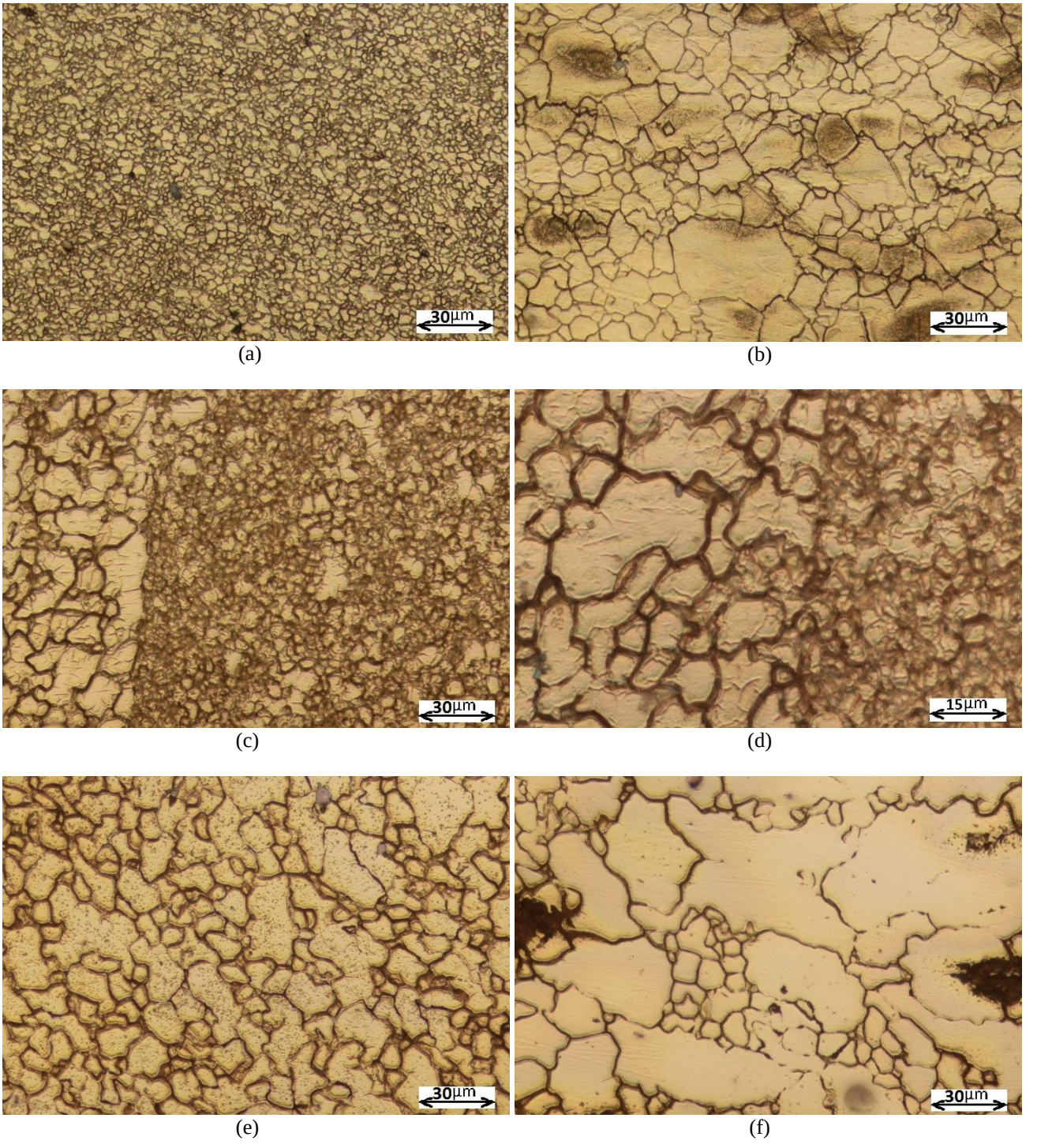

(a) (b)

(c) (d)

(e) (f)

Fig. 4 Metallography images (a) to (f) are A-1 test of the stir region, A-1 test of HAZ, A-2 tests of the stir region and HAZ (as c and d), A-6 test of the stir region, and A-6 test of HAZ, respectively.

Table 2 Hardness of samples in different transverse speeds and rotational speeds

Test number	Rotation Speed (rpm)	Transverse Speed (mm/min)	Hardness (Vicker)		
			HAZ	Interface	SZ
A-1	870	12	60.4	49.3	53.7
A-2	870	24	52.9	53.2	59.1
A-3	870	32	45.3	43.0	42.3
A-4	1140	12	43.6	51.2	48.4
A-6	1500	32	48.8	51.3	46.1

Zener-Hollomon parameter

This parameter is used for estimation of grain size and calculation of the grain refinement rate. Two important thermodynamic variables in FSP used in the Zener-Hollomon formula are the strain rate ε◦ (1/s) and the temperature peak T(K) leading to the identification of Z (1/s) according to the Eq. (1) [22]:

$$Z = \varepsilon^{\circ} \exp (Q/RT) \quad (1)$$

Where R is the constant of gases and Q is the activation energy. For AZ31 alloy, Q is equal to 135 KJ/mol (for self-diffusion) [22]. It should be noted that the least change in the value of Q affects Z values. The ultimate goal in researches performed was not to obtain the precise value of Z, but the systematic demonstration of the texture changes with a change in the thermodynamic parameters. Then, it can clearly be said that Z parameter is affected by the process inputs which are rotation and transverse speeds. For the estimation of Z parameter during FSP, first an estimation of the maximum average of temperature should be available. For this purpose, a thermal model presented for aluminium alloys, is employed as shown in Eq. (2) [22].

$$\frac{T}{T_m} = K\left(\frac{\omega^2}{2.262v \times 10^4}\right)^{\alpha} \quad (2)$$

Where T_m (◦C) is the melting temperature which is 606 (◦C) for the AZ31B magnesium alloy by using differential scanning calorimetry (DSC); and ω (rpm) and v (mm/s) are the rotational and transverse speeds of the tools during FSP, respectively. K and α are also the constants estimated to be equal to 0.494 and 0.083, respectively; they are extracted through matching the properties of AZ31 alloy reported in references [22]. Moreover, the average of strain rate (1/s) in stir zone during FSP is predictable using Eq. (3):

$$\varepsilon^{\circ} = \frac{\pi . \omega . r}{L} = 3.05 \times 10\text{-}2\ \omega \quad (3)$$

Where r and L are the mean radius and depth of stir region observed in FSP plane, respectively. Z parameter can be obtained as a function of ω and v by the use of Eq. (2) and Eq. (3). In addition to the Z parameter, pitch distance is also employed for the representation of FSP parameters. This concept is basically presented for the definition of input heat. The previous researches have shown that by an increase in the Z parameter, severe changes take place in the texture [22]. The results of the strain test in stir region are also dependent on the Z parameter. The greater the Z number, the more the yield strength is reduced, although toughness increases [22]. Table 3 shows the Z parameter, strain rate, and pitch distance for the performed tests.

Table 3 Summary of FSP parameters and estimated values for Zener-Hollomon parameter (Z)

ω (rpm)	V (mm/s)	Strain Rate (1/s)	Max. Temperature ℃	Z (1/s)
870	0.2	26.5	432	2.67×10^{11}
870	0.4	26.5	430	2.85×10^{11}
870	0.53	26.5	422	3.71×10^{11}
1140	0.2	34.8	479	8.3×10^{11}
1500	0.53	45.8	462	1.8×10^{11}

The second stage tests (compositing and change of the number of passes)

At this stage, a 1% CNT by weight was inserted inside the groove and after sealing the groove by pin-free tool, three samples were prepared. Then three tests were performed by different passes (passes 1, 2, and 3). The optical metallographic images of these three tests are shown in Fig. 5. With regard to the hardness of the initial raw sample (53.4 Brinell), and 69.0 Brinell in the stir region, 57.0 Brinell in the interface, and 53.4 Brinell in HAZ for the 3-pass sample, it can be said that in general, hardness in the 3-pass sample is increased. In addition to the 3-pass sample, a sample was also made in the 4-pass condition accompanied with hardness drop. It seems that due to high input heat in the 4-pass sample, the likelihood of the carbide compounds formation and destruction of CNTs is high [13]. On the other hand, mixing has not completely been done in the single-pass sample, since the sample surface is indicative of this fact after metallography.

As it is shown in Fig. 5, the single-pass sample has no homogeneity, where some homogeneity is observed in the 2-pass sample and it is clearly observed that mixing has not been completely done. Sample 3 has a suitable homogeneity which is clearly observable. The results of hardness test showed that the hardness of samples of 2-pass and 4-pass were nearly similar. Additionally, an increase in the number of passes not only increases the cost but it also results in more input heat and growth of

the grains in more distant regions. Therefore, the state of 3-pass was selected as a more suitable condition.

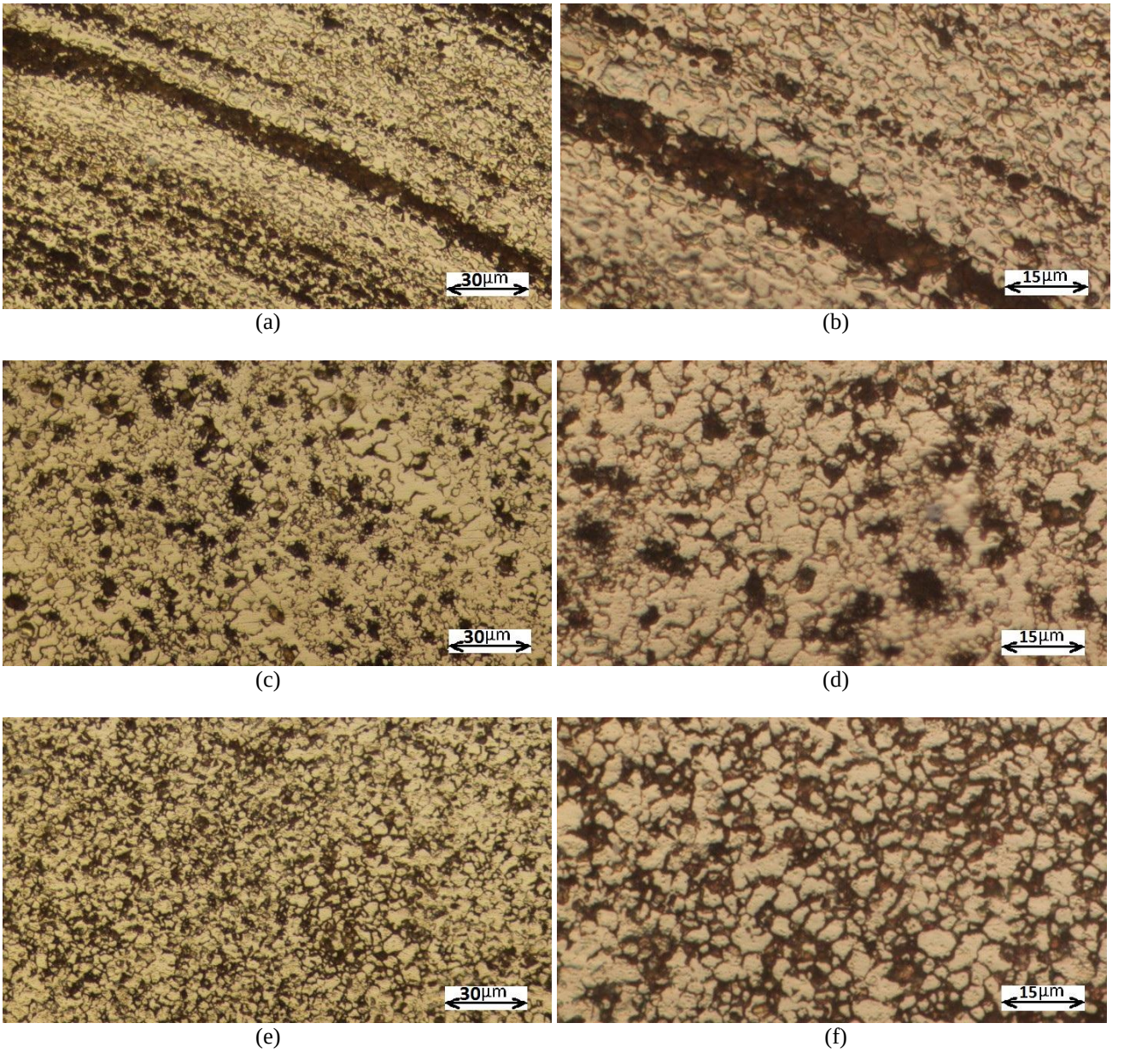

Fig. 5 Metallography images with different magnifications including images of (a) and (b) for single-pass sample, images of (c) and (d) for 2-pass sample, and images of (e) and (f) for 3-pass sample (at transverse speed of 870 rpm, 24 mm/min, 2-degree deviation angle, and right-turn direction).

The third stage tests (CNT percentage change)

For the weight fraction of CNTs in the composites at this stage, 0%, 1%, and 2% were selected. As it was mentioned before, a groove was made in samples. The depth of the groove in sample of 1% CNT weight was 2 millimetres and it was 4 millimetres for the 2% weight of CNT sample. The hardness of different regions is shown in Table 4 for these three samples. With a general view on Fig. 5 and Table 4, it can be said that by an increase in the number of passes and weight fraction of CNTs, the hardness of the weld region is improved. The more the number of passes, the more is the homogeneity of structure and the CNT agglomerations collapse. As a result, the reinforcement mechanism acts better compared with nano-scale (Orowan mechanism). Also, by an increase in CNT weight, the rate of reinforcing phase increases leading to an increase in strength.

Table 4 The hardness of the samples in different values of CNT (three-pass, 870rpm, 24 mm/min)

Weight percent of CNT	Vickers Hardness		
	Stir zone	Interface	Heat affected zone (HAZ)
0	53.1	53.9	41.9
1	62.3	60.9	51.6
2	66.1	57.6	61.6

Regarding the hardness of interface section, it can also be said that the fraction mixing of CNTs in this region has led to an increase in hardness. It seems that hardness in the base metal is decreased, but the value of reduction has been so much that the HAZ hardness has been more than that in SZ due to the effect of heat and the growth of the grains as depicted in samples 1 and 2. However, due to appropriate reinforcement in sample 3, the SZ hardness increases more than those of the two other regions.

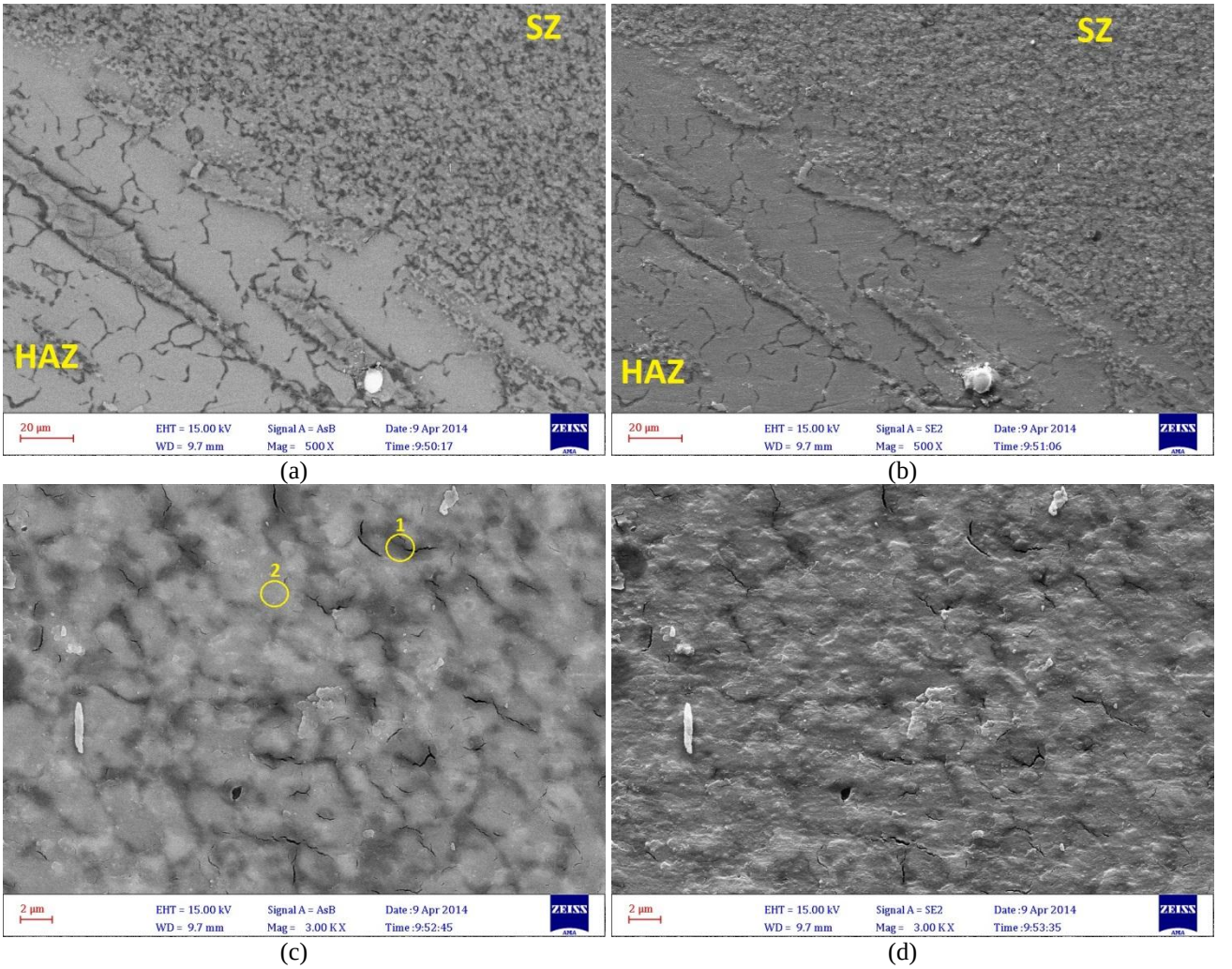

EDS 1

Element	Wt%	Error%
Mg	93.1	0.4
O	2.9	0.2
C	1.4	0.3
Al	1.4	0.4
Zn	1.2	0.3

(e)

EDS 2

Element	Wt%	Error%
Mg	76.7	0.6
O	15.2	0.6
C	5.8	0.3
Al	2.3	0.2

(f)

Fig. 6 Images of (a) and (b) show the SEM images of the interface region of the 3-pass sample with 1% CNT weight in two states of reversal and secondary electron; images of (c) and (d) show magnification higher than SZ in two states of reversal and secondary electron; and images of (d) and (e) show the EDS analyses of the yellow circles of (1) and (2) inside image (c), respectively.

Fig. 6 shows the SEM images and EDS analyses of the 3-pass composite sample. Image (a), which is a backscattered (BS) electron state, clearly shows the homogenization of the microstructure and more uniform distribution of elements in the stir region. In image (b) and in the HAZ, oxide region remains in the form of islands resulting from their oxide nature and their higher resistance against corrosion. These islands are well homogenized in the stir region. Images (c) and (d) also show the higher magnifications of SZ which is more homogenous both from the view of the distribution of the elements (BS electron state) as well as surface morphology and surface uniform corrosion (secondary electron state).

The EDS analyses are also indicative of an increase in carbon percentage in the background. What is clear, however, is the fact that some CNT agglomerates remained (especially from the EDS analysis of circle 2 in Fig. 6 (c). That is because an increase of 5% carbon cannot result from the even distribution. Anyhow, with regard to what was stated and the study of mechanical properties, the 3-pass state demonstrates very good results in addition to the fact that there is more even distribution of the elements with grain size less than before.

4 CONCLUSION

- This research embarked on the study of surface compositing of AZ31B magnesium with CNT by FSP method. The parameters under study were rotational speed, transverse speed, number of passes, and weight fraction of CNTs.
- Suitable limits for transverse speed and rotational speed were identified to be 12-24 mm/min and 870-1140 rpm, respectively. The highest hardness in the process of surface compositing was seen at the transverse speed of 24 mm/min and rotational speed of 870 rpm with a hardness of about 60 Vickers and the grain size of less than 5 μm in the stir region.
- The Zener-Holloman parameter was calculated for the tests and the least value was related to the conditions of the transverse speeds of 12-24 mm/min and rotational speed of 870 rpm. As a result, the samples with the finest grains were experimentally and theoretically specified.
- The effect of the number of passes (1, 2, and 3) was investigated for compositing, revealing the most homogenous structure of the 3-pass state with the highest hardness of 69 Vickers.
- 2% was the best weight rate for CNTs accompanied with the highest hardness. Performance of the 3-pass of process properly distributed the CNTs in the matrix.

5 REFERENCES

[1] Zhang, D. T., Xiong, F., Zhang W. W., Qui, C., and Zhang, W., "Superplasticity of AZ31 Magnesium Alloy Prepared by Friction Stir Processing", Transactions of Nonferrous Metals Society of China, Vol. 21, 2011, pp. 1911-1916.

[2] Gray, J. E., Luan, B., "Protective Coatings on Magnesium and Its Alloys: A Critical Review", Journal of Alloys and Compounds, Vol. 336, 2002, pp. 88-113.

[3] Lim, D. K., Shibayanagi, T., and Gerlich, A. P., "Synthesis of Multi-Walled CNT Reinforced Aluminium Alloy Composite via Friction Stir Processing", Materials Science and Engineering A, Vol. 507, 2009, pp. 194-199.

[4] Woo, W., Choo, H., Brown, D. W., Liaw, P. K., and Feng, Z., "Texture Variation and Its Influence on the Tensile Behavior of a Friction-Stir Processed Magnesium Alloy", Scripta Materialia, Vol. 54, 2006, pp. 1859-1864.

[5] Darras, B. M., "A Model to Predict the Resulting Grain Size of Friction-Stir-Processed AZ31 Magnesium Alloy", Journal of Materials Engineering and Performance, Vol. 21, No. 7, 2012, pp. 1243-1248.

[6] Du, X. H., Wu, B.L., "Using Two-Pass Friction Stir Processing to Produce Nanocrystalline Microstructure in AZ61 Magnesium Alloy", Science in China Series E: Technological Sciences, Vol. 52, No.6, 2009, pp. 1751-1755.

[7] Woo, W., Choo, H., Prime. M. B., Feng, Z., and Clausen, B., "Microstructure, Texture and Residual Stress in a Friction-Stir-Processed AZ31B Magnesium Alloy", Acta Materialia, Vol 56, 2008, pp. 1701-1711.

[8] Faraji, G., Dastani, O., and Akbari Mousavi, S. A. A., "Effect of Process Parameters on Microstructure and Micro-Hardness of AZ91/Al_2O_3 Surface Composite Produced by FSP", Journal of Materials Engineering and Performance, Vol. 20, No. 9, 2011, pp. 1583-1590.

[9] Asadi, P., Faraji, G., and Besharati, M. K., "Producing of AZ91/SiC Composite by Friction Stir Processing (FSP)", International Journal of Advanced Manufacturing Technology, Vol. 51, 2010, pp. 247-260.

[10] Asadi, P., Faraji, G., Masoudi, A., and Besharati Givi, M. K., "Experimental Investigation of Magnesium-Based Nanocomposite Produced by Friction Stir Processing: Effects of Particle Types and Number of Friction Stir Processing Passes", Metallurgical and Material Transactions A, Vol. 42A, 2011, pp. 2820-2832.

[11] Lee, C. J., Huang, J. C., and Hsieh, P. J., "Mg Based Nano-Composites Fabricated by Friction Stir Processing", Scripta Materialia, Vol. 54, 2006, pp. 1415–1420.

[12] Izadi, H., Gerlich, A. P., "Distribution and Stability of Carbon Nanotubes during Multi-Pass Friction Stir Processing of Carbon Nanotube/Aluminum Composites", Carbon, Vol. 50, 2012, pp. 4744-4749.

[13] Johannes, L. B., Yowell, L. L., Sosa, E., Arepalli, S., and Mishra, R. S., "Survivability of Single-Walled

Carbon Nanotubes during Friction Stir Processing", Nanotechnology, Vol. 17, 2006, pp. 3081-3084.

[14] Liu, Q., Ke, L., Liu, F., Huang, C., and Xing, Li., "Microstructure and Mechanical Property of Multi-Walled Carbon Nanotubes Reinforced Aluminum Matrix Composites Fabricated by Friction Stir Processing", Materials and Design, Vol. 45, 2013, pp. 343-348.

[15] Housh, S., Mikucki, B., "Properties and Selection: Nonferrous Alloys and Special-Purpose Materials: Selection and Application of Magnesium and Magnesium Alloys", United States of America: ASM International, ASM Handbook, Vol. 2, 1990, Chap. 1.

[16] Becherer, B. A., Witheford, T. J., "Heat Treating: Heat Treating of Ultrahigh-Strength Steels", United States of America: ASM International, ASM Handbook, Vol. 4, 1991, Chap. 1.

[17] Azizieh, M., Kokabi, A. H., and Abachi, A., "Effect of Rotational Speed and Probe Profile on Microstructure and Hardness of AZ31/Al_2O_3 Nanocomposites Fabricated by Friction Stir Processing", Materials and Design, Vol. 32, 2011, pp. 2034-2041.

[18] Yu, Z., Zhang, W., Choo, H., and Feng, Z., "Transient Heat and Material Flow Modelling of Friction Stir Processing of Magnesium Alloy Using Threaded Tool", Metallurgical and Materials Transactions A, Vol. 43, 2011, pp. 724-737.

[19] Alavi Nia, A., Omidvar, H., and Nourbakhsh, S. H., "Investigation of the Effects of Thread Pitch and Water Cooling Action on the Mechanical Strength and Microstructure of Friction Stir Processed AZ31", Materials & Design, Vol. 52, 2013, pp. 615-620.

[20] Chang, C. I., Du, X. H., and Huang, J. C., "Producing Nanograined Microstructure in Mg–Al–Zn Alloy by Two-Step Friction Stir Processing", Scripta Materialia, Vol. 59, No. 3, 2008, pp. 356-359.

[21] Chang, C. I., Du, X. H., and Huang, J. C., "Achieving Ultrafine Grain Size in Mg–Al–Zn Alloy by Friction Stir Processing", Scripta Materialia, Vol. 57, No. 3, 2007, pp. 209-212.

[22] Yu, Z., Choo, H., Feng, Z., and Vogel, S. C., "Influence of Thermo-Mechanical Parameters on Texture and Tensile Behavior of Friction Stir Processed Mg Alloy", Scripta Materialia, Vol. 63, No. 11, 2010, pp. 1112-1115.